PLK1 regulates both ASAP localization and its role in spindle pole integrity.

G. Eot-Houllier, M. Venoux, S. Vidal-Eychenié, Mt Hoang, D. Giorgi, Sylvie Rouquier

THE JOURNAL OF BIOLOGICAL CHEMISTRY VOL. 285, NO. 38, pp. 29556–29568, September 17, 2010

Plk1 Regulates Both ASAP Localization and Its Role in Spindle Pole Integrity*[S]

Received for publication, May 17, 2010, and in revised form, July 2, 2010 Published, JBC Papers in Press, July 8, 2010, DOI 10.1074/jbc.M110.144220

Grégory Eot-Houllier[1], Magali Venoux[2], Sophie Vidal-Eychenié, Minh-Thâo Hoang, Dominique Giorgi, and Sylvie Rouquier[3]

From the Groupe Microtubules et Cycle Cellulaire, Institut de Génétique Humaine, CNRS UPR 1142, rue de la Cardonille, 34396 Montpellier Cédex 5, France

Bipolar spindle formation is essential for faithful chromosome segregation at mitosis. Because centrosomes define spindle poles, abnormal number and structural organization of centrosomes can lead to loss of spindle bipolarity and genetic integrity. ASAP (*a*ster-*a*ssociated *p*rotein or MAP9) is a centrosome- and spindle-associated protein, the deregulation of which induces severe mitotic defects. Its phosphorylation by Aurora A is required for spindle assembly and mitosis progression. Here, we show that ASAP is localized to the spindle poles by Polo-like kinase 1 (Plk1) (a mitotic kinase that plays an essential role in centrosome regulation and mitotic spindle assembly) through the γ-TuRC-dependent pathway. We also demonstrate that ASAP is a novel substrate of Plk1 phosphorylation and have identified serine 289 as the major phosphorylation site by Plk1 *in vivo*. ASAP phosphorylated on serine 289 is localized to centrosomes during mitosis, but this phosphorylation is not required for its Plk1-dependent localization at the spindle poles. We show that phosphorylated ASAP on serine 289 contributes to spindle pole stability in a microtubule-dependent manner. These data reveal a novel function of ASAP in centrosome integrity. Our results highlight dual ASAP regulation by Plk1 and further confirm the importance of ASAP for spindle pole organization, bipolar spindle assembly, and mitosis.

Centrosomes are the primary microtubule (MT)[4]-organizing centers in most vertebrate cells. During interphase, they organize a MT array that imparts shape and polarity to the cell. During mitosis, they contribute to the assembly of the mitotic spindle, which is based on a bipolar array of highly dynamic MTs that ensures accurate chromosome segregation (for reviews, see Refs. 1 and 2). Equal segregation of genetic material between daughter cells requires the mitotic spindle to be bipolar, and the formation of monopolar or multipolar spindles leads to abnormal segregation. Centrosomes consist of two centrioles that are barrel-shaped structures made of MT bundles and surrounded by electron-dense pericentriolar material (PCM), the main site for MT nucleation. At the G_2/M transition, centrosomes undergo maturation during which the PCM expands through the recruitment of the MT nucleator γ-tubulin ring complex (γTuRC), resulting in increased MT nucleation activity (3). γTuRC is recruited to centrosomes via its component NEDD1/GCP-WD (4, 5), where γ-tubulin promotes the polymerization of α/β-tubulin subunits into MT polymers. The exact execution of both the centrosome cycle and function lies behind the correct formation of bipolar spindles that, in turn, allows faithful chromosome segregation. Deregulation of these events could impair accurate inheritance of genetic material. Indeed, the precise distribution of the duplicated chromosomes to the daughter cells is crucial because aberrant cell division leads to genetic diseases and aneuploidy, a hallmark of cancer cells (6).

The Ser/Thr mitotic kinases Aurora A and Polo-like kinase 1 (Plk1) are considered key regulators of centrosome maturation in different organisms (2, 7–9). Their deregulation has been linked to centrosome abnormalities, drug resistance, and oncogenesis (10). Plk1 belongs to the mammalian Plk family that comprises four members (Plk1–Plk4). Plk1 is involved in a variety of mitotic events, including G_2/M transition, centrosome maturation and separation, mitotic spindle formation, chromosome segregation, and cytokinesis (7, 11, 12). Plk1 is dynamically expressed in various mitotic structures as cells progress through the different stages of mitosis (7), and many Plk1 substrates have been identified that could explain its diverse functions in cell division (12). During interphase and early prophase, Plk1 is found at centrosomes, where it facilitates γ-tubulin recruitment, centrosome maturation and separation, as well as microtubule nucleation during late prophase and prometaphase (13). Inhibition of Plk1 function prevents the recruitment of γ-tubulin to mitotic centrosomes and also the centrosomal nucleation pathway. Plk1 phosphorylation of NEDD1 is required for targeting γ-TuRC to ensure centrosome maturation (14–16).

Plk1 is composed of an N-terminal catalytic domain, which is conserved among the members of the Plk family, and a relatively divergent C-terminal regulatory domain that contains two polo boxes and it is therefore called the Polo box domain

* This work was supported by the CNRS and Association pour la Recherche contre le Cancer Grant 4027 (to S. R.), Ligue Nationale contre le Cancer Grants Comité de l'Hérault-2007 and Comité de l'Aude-2009 (to S. R.), and by the Fondation Jérôme Lejeune (S. R.).

[S] The on-line version of this article (available at http://www.jbc.org) contains supplemental Figs. S1–S6.

[1] Supported by postdoctoral fellowships from the Institut National du Cancer (France) (2008) and the Ligue Nationale contre le Cancer (2009).

[2] Supported by fellowships from Ministère de l'Enseignement de la Recherche et de la Technologie and the Association pour la Recherche contre le Cancer.

[3] To whom correspondence should be addressed. Fax: 33-499619935; E-mail: rouquier@igh.cnrs.fr.

[4] The abbreviations used are: MT, microtubule; ASAP, aster-associated protein; γTuRC, γ-tubulin ring complex; KD, kinase dead; MAP, microtubule-associated protein; MTSB, microtubule stabilization buffer; PBD, Polo box domain; PCM, pericentriolar material; Plk1, Polo-like kinase 1; TAL, ZK-thiazolidinone.

(PBD). In the absence of a bound ligand, the PBD inhibits the basal kinase activity of Plk1 via intramolecular interactions with the kinase domain. A model has been proposed, in which PBD binding to phosphorylated substrates primed by another kinase (Cyclin-dependent kinases, Cdks, and/or Plks) releases the kinase domain and simultaneously localizes Plk1 to specific subcellular structures (17–19). However, it has recently been shown that the priming phosphorylation is not needed for all interactions between Plk1 and its targets (20, 21). These findings suggest that Plk1 can also interact with some of its ligands through a phospho-independent or PBD-independent mechanism and that, therefore, PBD-dependent interactions are likely to be more divergent than originally conjectured (22).

We have recently characterized the spindle- and centrosome-associated protein ASAP (*A*ster-*A*ssociated *P*rotein or MAP9) that is phosphorylated by Aurora A and plays a key role in spindle assembly and mitotic progression. Deregulated ASAP expression leads to abnormal spindles and chromosome congression and segregation defects that result in aneuploidy and/or cell death (23). Phosphorylation of ASAP by Aurora A on Ser-625 is required for bipolar spindle assembly and is essential for correct mitotic progression (24). Recent findings have highlighted a functional cross-talk between Aurora A and Plk1 in which Aurora A is responsible for the initial phosphorylation and activation of Plk1 at the G_2/M transition (21, 25–27), and Plk1 is promoting activation of Aurora A (28). Because ASAP is a mitotic substrate of Aurora A, we therefore investigated whether ASAP could functionally interact with Plk1 as well.

Here, we report that ASAP is recruited to the centrosome and to the spindle by Plk1 through the NEDD1-γ-tubulin pathway and that it is a novel substrate of Plk1 kinase. We identified serine 289 as a major phosphorylation site for Plk1 *in vivo*. We demonstrate that Plk1-mediated phosphorylation of ASAP occurs at centrosomes and is involved in spindle pole stabilization during mitosis but not in ASAP localization. We thus highlight ASAP as a new factor contributing to centrosome integrity and confirm that it is a key component of the mitotic apparatus because it is required for normal progression of mitosis in mammalian cells.

MATERIALS AND METHODS

Plasmids and Constructs—Cloning was carried out using standard PCR-based techniques. Mutagenesis was performed using the Multisite-directed Mutagenesis kit from Stratagene. For production of recombinant proteins, wild type Plk1 (Plk1-WT) and the kinase-dead N281A mutant (Plk1-KD) cDNAs were subcloned into the pRSETC vector (Invitrogen) to produce His_6-tagged proteins (His_6-Plk1-WT and His_6-Plk1-KD). The pRC-MYC-Plk1-WT plasmid (Myc-Plk1-WT) was kindly provided by Dr R. H. Medema and is described in Ref. 29. The PBD mutant H538A/K540M (Myc-Plk1-PBD mut) and the Myc-Plk1-KD constructs were derived from the pRC-MYC-Plk1-WT plasmid by mutagenesis. FLAG-tagged ASAP and YFP-ASAP fusion proteins were described in Ref. 23. FLAG-ASAP-S289A and YFP-ASAP-S289A/E were derived by mutagenesis. Full-length ASAP (GST-ASAP-WT) and the six GST-ASAP constructs (G1, amino acids 1–108; G2, 75–206; G3, 187–313; G4, 296–420; G5, 395–563; and G6, 544–647) were described in Ref. 24. All constructs were fully sequenced.

Chemicals and Reagents—Thymidine, nocodazole, Taxol, and roscovitine were purchased from Sigma. RO-3306 was purchased from Calbiochem. The Plk1 inhibitor ZK-thiazolidinone (TAL) was described in Ref. 30 and kindly provided by Bayer Schering Pharma AG. MLN8054 was described in Ref. 36 and kindly provided by Millennium Pharmaceutical, Inc.

Purification of Recombinant Proteins—His_6-Plk1-WT and His_6-Plk1-KD were expressed in *Escherichia coli* strain C43 and purified under native conditions using standard protocols (QIAexpressionist System; Qiagen). The GST-ASAP fusion proteins were expressed in the *E. coli* strain BL21RP$^+$ and purified using glutathione-agarose resin (Sigma) following the manufacturer's guidelines. Cdk1/Cyclin B recombinant proteins were purchased from Upstate.

Antibodies—The following rabbit polyclonal antibodies were used: anti-ASAP (23), anti-NEDD1 (4), anti-Cdc27 (31), anti-γ-tubulin (AK-15; Sigma), anti-Pericentrin (ab4448; Abcam), and anti-actin (20-33; Sigma). Mouse monoclonal antibodies were: anti-ASAP (6G5) (24), anti-Plk1 (ab17057; Abcam), anti-α-tubulin (DM1A; Sigma), anti-γ-tubulin (GTU-88; Sigma), anti-TPX2 (18D5; BioLegend), anti-phosphohistone H3 (Ser-10) (6G3; Cell Signaling Technology), anti-Centrin (provided by Dr. J. Salisbury (Mayo Clinic, Rochester, MN)), and anti-Myc tag (ab32; Abcam). The concentrations of the different antibodies used for Western blotting, immunofluorescence, or immunoprecipitation are available on request.

The anti-phosphoserine 289 ASAP (Ser(P)-289) antibody was obtained by immunizing rabbits with the DENKENpSFSADH peptide coupled to peptide KHL. Antibodies were produced and affinity chromatography-purified by Eurogentec (Belgium). The purification procedure involved two successive steps using the phosphorylated and nonphosphorylated forms of the peptide. Ser(P)-289 was diluted to 1/500 for Western blotting or immunofluorescence experiments.

Cell Culture and Transfections—U-2 OS cells were routinely grown at 37 °C in a 5% CO_2 atmosphere in DMEM (Lonza) supplemented with 10% fetal calf serum, 0.3 g/liter L-glutamine, 0.05 g/liter streptomycin, and 50,000 units/liter penicillin. For short interfering RNA (siRNA) experiments, cells were transfected with 30 nM siRNA duplexes using the Hiperfect reagent (Qiagen) as described in Ref. 24. siRNAs against *ASAP* (5′-CGCCGAAUGGCAUACAAUUTT-3′), *Plk1* (5′-CGAGCUGCUUAAUGACGAG-3′), *NEDD1* (5′-GCAGACAUGUGUCAAUUUATT-3′), and control Luciferase *GL2* (siGL2, 5′-CGUACGCGGAAUACUUCGATT-3′) were purchased from Eurofins MWG Operon (Germany). The siRNA against *γ-tubulin* was the validated siRNA Hs_TUBG1_5_HP from Qiagen. Plasmids were transfected using the JetPei reagent (Polyplus; Ozyme) according to the manufacturer's guidelines. For rescue experiments, 50 ng of YFP-ASAP (WT or mutants) plasmids together with the pCDNA vector to a final concentration of 1.5 μg of DNA were transfected with JetPei 16 h after siRNA transfection, and cells were then grown for 48 h. Where indicated, MT depolymerization was performed on ice for 60 min. Where indicated, cells were synchronized by thymidine block (2 mM) for 24 h, released by two washes in PBS, and

analyzed at S, G_2, or M phase. To synchronize cells in M phase for ASAP-Plk1 co-immunoprecipitation experiments, cells were subjected to double thymidine block (2 mM): first block for 22 h, release for 14 h, and second block for 16 h. Cells were harvested 13 h after the second release.

For drug treatment, cells were transfected with 1 μg of FLAG-ASAP plasmids for 24 h. After synchronization by thymidine block and release with 20 ng/ml nocodazole for 16 h, mitotic cells were collected by shake-off and incubated with 50 μM roscovitine or 2 μM RO-3306, or 1 μM TAL (Plk1 inhibitor) or 10 μM MLN8054 (Aurora A inhibitor) for another 30 min. Where indicated, for the Plk1 inhibitor, after synchronization by thymidine block, cells were released in the presence of 1 μM TAL for 13 h. Modifications of these procedures were introduced in some experiments, and in that case they are indicated in the figure legends.

Immunoblotting—Whole cell extracts were obtained by scraping and boiling U-2 OS cells in SDS sample buffer. Extracts were separated by SDS-PAGE and transferred to nitrocellulose or PVDF membranes as described previously (23). Blots were incubated with primary antibodies at 4 °C overnight, and antibody binding was detected using the Super Signal kit from Pierce (Perbio). Sample loading was controlled with anti-α-tubulin or anti-Actin antibodies (diluted 1/10,000).

Immunoprecipitations—Co-immunoprecipitation experiments were performed either with cells co-transfected with the indicated plasmids or with the endogenous proteins from mitotic extracts. Synchronized mitotic cells were collected about 14 h after the release from the thymidine block. Total cell extracts or mitotic cells extracts were immunoprecipitated following standard procedures as described (24) in 40 mM Tris, pH 7.6, 150 mM NaCl, 1 mM EDTA, 1 mM EGTA, 0.5% Nonidet P-40, and 0.25% Triton X-100 for co-immunoprecipitation of ASAP-Plk1; in 40 mM Tris, pH 7.6, 150 mM NaCl, 5 mM EGTA, and 0.5% Nonidet P-40 for co-immunoprecipitation of ASAP-γ-tubulin. All immunoprecipitation buffers were complemented with 1 mM DTT, 2 mM Na_3VO_4, 10 mM NaF, 10 mM β-glycerophosphate, and protease inhibitor mixture (Roche Diagnostics). Lysates were incubated with the indicated antibodies overnight and then at 4 °C for 1 h with 10 μl of magnetic Dynabeads-protein G beads, which had been first saturated at 4 °C in the lysis buffer and 1% BSA for 1 h. After three washes in the same buffer, bound proteins were eluted in 10 μl of 2× Laemmli sample buffer. Proteins were separated on SDS-PAGE and then immunoblotted with the corresponding antibodies as indicated.

For λ-phosphatase treatment, FLAG-ASAP-WT was expressed in U-2 OS cells. Cells were immunoprecipitated with the anti-ASAP antibody and treated with 600 units of λ-phosphatase (New England Biolabs, Ozyme) at 30 °C for 60 min. Proteins were then separated on 8% polyacrylamide gels and transferred to nitrocellulose membranes before Western blotting with the anti-Ser(P)-289 antibody.

Immunofluorescence—Cells grown on coverslips were fixed either with 4% paraformaldehyde in microtubule stabilization buffer (MTSB: 100 mM Pipes, 1 mM EGTA, 4% PEG 8000, pH 6.9) at room temperature for 10 min followed by permeabilization in 0.5% Triton X-100/MTSB for 5 min (PAF/MTSB fixation) or with 3.6% formaldehyde in PHEM (60 mM Pipes, 25 mM Hepes, 10 mM EGTA, 2 mM $MgCl_2$, pH 6.9) for 10 min followed by permeabilization in methanol at room temperature for 1 min (F/PHEM/methanol fixation). Fixed cells were incubated at 37 °C with the primary antibodies for 1 h and with the secondary antibodies (Alexa Fluor 488- and 555-conjugated goat anti-rabbit or anti-mouse immunoglobulins G (IgGs) (1/1,000; Invitrogen)) at 37 °C for 30 min. All antibodies were diluted in PBS/3% BSA. Coverslips were mounted using Gel-Mount (Biomeda). Images were acquired using a Leica DM6000B wide field or a Nikon A1R confocal microscope and CCD cameras and processed with the Metamorph or NIS-Elements AR 3.0 software, respectively.

In Vitro Kinase Assays—All Plk1 *in vitro* kinase assays were performed in kinase buffer (20 mM Hepes, pH 7.5, 150 mM KCl, 10 mM $MgCl_2$, 1 mM EGTA, 1 mM DTT, 5 mM NaF, 0.2 mM Na_3VO_4, protease inhibitor mixture) supplemented with 100 μM ATP and 10 μCi of [γ-^{32}P]ATP (3,000 Ci/mmol; Amersham Biosciences) at 30 °C for 30 min in the presence of 1.5 μg of the indicated bacterially expressed GST fusion proteins or 1 μg of dephosphorylated α-casein (Sigma). Reactions were stopped by adding gel sample buffer and analyzed by SDS-PAGE and autoradiography. For two-step sequential protein phosphorylation assays, GST-ASAP (WT or mutants) was first incubated in 20 μl of kinase buffer with or without 100 ng of Cdk1/Cyclin B at 30 °C in the presence of 1 mM ATP for 30 min. After inhibition of Cdk1 by adding 2 μM RO-3306 for 10 min, GST-ASAP (WT or mutants) was further incubated with 1 μg of Plk1 in 30 μl (final volume) at 30 °C for 30 min. Reactions were stopped with gel sample buffer and analyzed by Western blotting with the indicated antibodies.

Phosphoamino Acid Analysis and Phosphopeptide Mapping—Phosphoamino acid analysis of *in vitro* phosphorylated ASAP was performed by acid hydrolysis and high voltage two-dimensional electrophoresis on high performance thin layer cellulose plates as described (24). Phosphopeptide mapping of full-length in *vitro* phosphorylated recombinant ASAP was performed by mass spectrometry as described (24). Briefly, protein bands were excised from gels and cut into ~1-mm^3 pieces. Gel pieces were then subjected to in-gel trypsin digestion. Samples were injected in a nanoscale reversed phase HPLC capillary column (75 μm × 10^{-12} cm) coupled on-line with an LTQ linear ion-trap mass spectrometer (ThermoElectron; San Jose, CA). Eluting peptides were detected, isolated, and fragmented to produce a tandem mass spectrum of specific fragment ions for each peptide. Peptide sequences (and hence protein identity) were determined by matching protein with the acquired fragmentation pattern using the software program MASCOT (Matrix Science). The modification of 80 mass units to serine, threonine, and tyrosine was included in the database searches to identify the phosphopeptides. Each phosphopeptide that was determined by the MASCOT program was also inspected manually to ensure confidence.

Centrosome Preparations—Centrosomal fractions from U-2 OS cells were purified using a sucrose gradient according to the original protocol developed by Moudjou (32). Briefly, 1×10^7 to 3×10^7 U-2 OS cells, treated previously with cytochalasin D and nocodazole, were harvested by trypsinization, washed in a

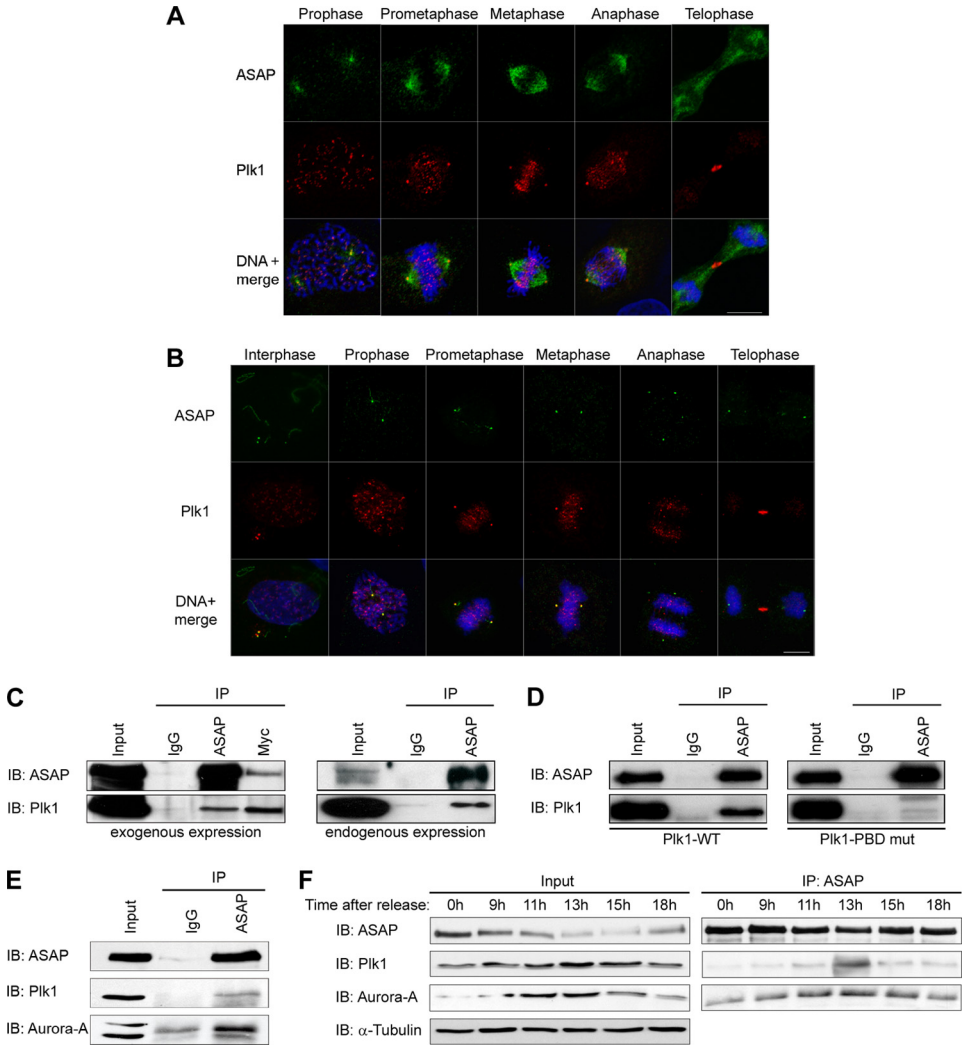

FIGURE 1. **ASAP and Plk1 co-localize at centrosomes and interact *in vivo* during mitosis.** *A* and *B*, asynchronous U-2 OS cells were grown on glass coverslips and fixed in PAF/MTSB (*A*) or F/PHEM/methanol (*B*) (see "Materials and Methods") and labeled with the polyclonal anti-ASAP (*green*), or the monoclonal anti-Plk1 antibodies (*red*) and stained with Hoechst 33258 (*blue*) without (*A*) or after (*B*) depolymerization of MTs by incubation on ice for 60 min. The different stages of the cell cycle are shown from prophase (*A*) or interphase (*B*) to telophase (*scale bar*, 10 μm). *C*, U-2 OS cell lysates were immunoprecipitated (*IP*) with rabbit IgG, rabbit anti-ASAP, or anti-Myc antibodies, and the precipitates were analyzed by immunoblotting (*IB*) with antibodies against ASAP or Plk1. *Left*, asynchronous cells were co-transfected with FLAG-ASAP and Myc-Plk1 (*Input*, 10% of protein extracts; immunoprecipitated with 200 μg of protein extracts). *Right*, endogenous proteins were co-immunoprecipitated from synchronized mitotic cells (see "Materials and Methods") (*Input*, 10% of protein extracts; immunoprecipitated with 2 mg of protein extracts). A higher exposure is shown for Plk1 immunoblot. See supplemental Fig. S1*A* for uncropped gels. *D*, asynchronous U-2 OS cells were transfected with FLAG-ASAP and either Myc-Plk1-WT (*left*) or Myc-Plk1-PBD mutant (*mut*) (*right*) and immunoprecipitated with rabbit IgG or rabbit anti-ASAP antibody. Precipitates were analyzed by immunoblotting with antibodies against ASAP or Plk1. See supplemental Fig. S1*B* for uncropped gel. *E*, U-2 OS cells were transfected with FLAG-ASAP, and 24 h later, cell lysates were immunoprecipitated with rabbit IgG or rabbit anti-ASAP antibodies (*Input*, 10% of protein extracts immunoprecipitated with 200 μg of protein extracts). Precipitates were analyzed by immunoblotting with antibodies against ASAP, Plk1, or Aurora A. See supplemental Fig. S1*C* for uncropped gel. *F*, FLAG-ASAP-transfected cells were arrested at the G_1/S boundary by thymidine block (2 mM for 24 h) and then released into fresh medium. Samples harvested at the indicated time points were analyzed by immunoblotting using antibodies against ASAP, Plk1, or Aurora A. Inputs are shown on the *left* and immunoprecipitates on the *right*. α-Tubulin was used as a loading control.

half-volume of TBS, 10-fold diluted in TBS containing 8% sucrose, and then lysed in a 5-ml solution of 1 mM Hepes, pH 7.2, 0.5% Nonidet P-40, 500 μM $MgCl_2$, 0.1% 2-mercaptoethanol complemented with the Complete Protease Inhibitor Mixture (Roche Diagnostics), 1 mM Na_3VO_4, and 50 mM NaF phosphatase inhibitors. 10 mM Hepes (final concentration) and 1 μg/ml DNase I (Roche Diagnostics) were added to the cleared lysates (2,500 $\times$ *g* for 10 min) and incubated on ice for 30 min. Centrosomes were sedimented into a 0.5-ml cushion of 60% sucrose (in 10 mM Pipes, pH 7.2, 0.1% Triton X-100, 0.1% 2-mercaptoethanol) by centrifugation at 10,000 $\times$ *g* for 30 min. The interface layer as well as the sucrose cushion were further purified through a discontinuous sucrose gradient consisting of 500 μl of 70%, 300 μl of 50%, and 300 μl of 40% sucrose solutions and centrifuged at 40,000 $\times$ *g* for 1 h. Fractions were collected from the bottom (200 μl/fraction, from fractions 1 to 8; the remaining solution was collected as fraction 9). A small aliquot of each fraction was sedimented onto round coverslips in tubes containing a special Plexiglas adapter and then immunostained using anti-γ-tubulin antibodies to estimate the centrosome yield in each fraction and anti-ASAP antibodies. Each fraction was diluted in 1 ml of 10 mM Pipes buffer, pH 7.2, and centrosomes were recovered by centrifugation at 15,000 $\times$ *g* for 10 min and boiled in SDS sample buffer.

RESULTS

ASAP Co-localizes and Interacts with Plk1—To determine whether ASAP interacts with Plk1, we first investigated ASAP spatiotemporal expression relative to Plk1 during the cell cycle in U-2 OS cells by immunofluorescence analysis. As already described, Plk1 localized to centrosomes and kinetochores from G_2 to anaphase and at the midbody during anaphase, whereas ASAP localized to centrosomes throughout the cell cycle and to the mitotic and central spindle (Fig. 1, *A* and *B*). Thus, ASAP and Plk1 co-localize at centrosomes from G_2 to telophase (Fig. 1*B*). We then performed co-immunoprecipitation experiments to assess whether ASAP and Plk1 interact *in vivo*. ASAP was co-precipitated with Plk1 in U-2 OS cells that had been transfected with FLAG-ASAP-WT and Myc-Plk1-WT (Fig. 1*C*, *left panel*, and supplemental Fig. S1*A*), and immunoprecipitation of endogenous ASAP revealed its association with Plk1 in mitotic synchronized cells (Fig. 1*C*, *right panel*, and supplemental Fig. S1*B*). In agreement with previous studies suggesting that Plk1 stably interacts with its tar-

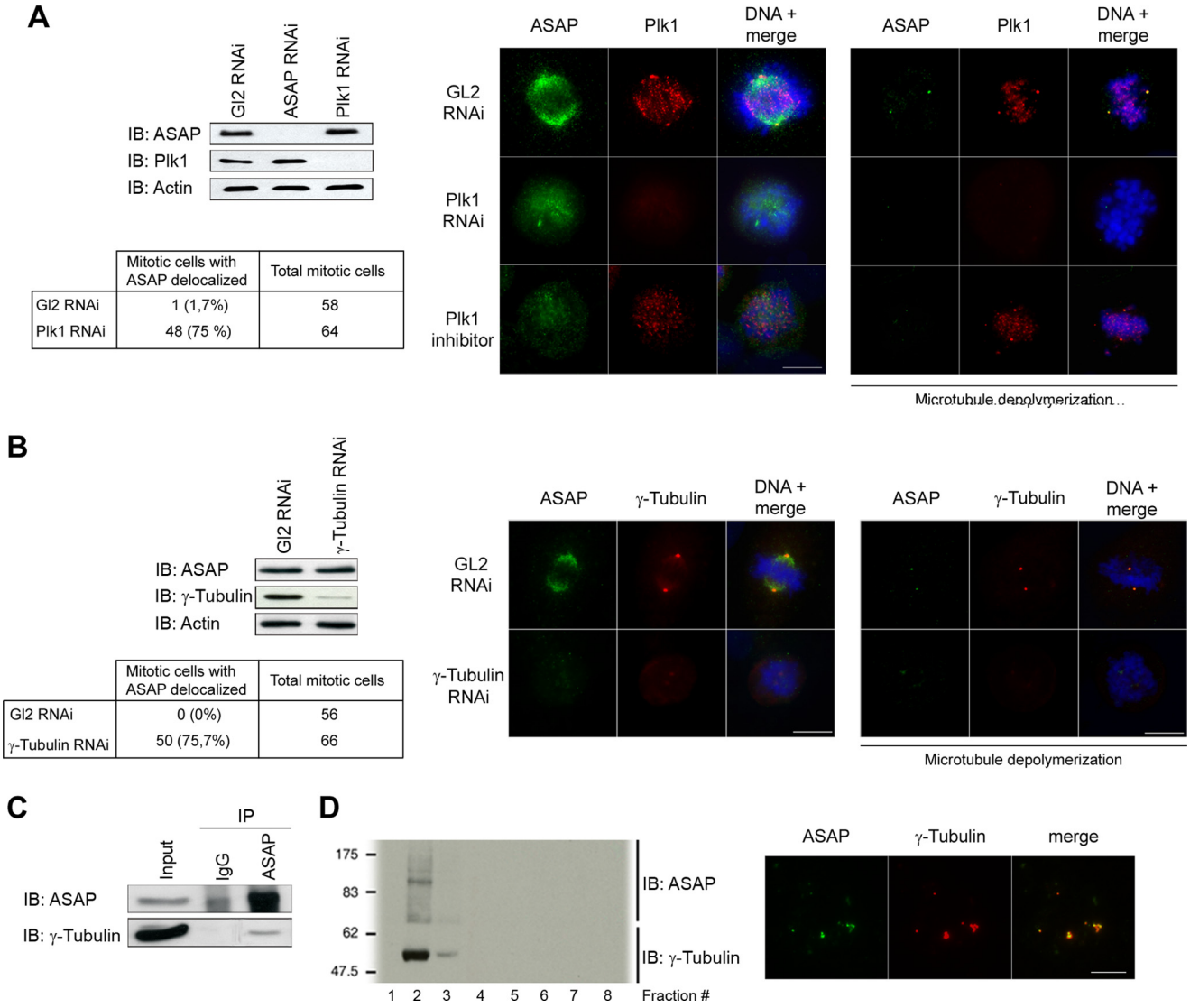

FIGURE 2. **Plk1 promotes ASAP localization to centrosomes and spindles through the NEDD1-γ-tubulin pathway.** *A*, asynchronous U-2 OS cells were transfected with *Luciferase GL2* (control), *ASAP*, or *Plk1* siRNAs. Cell extracts were immunoblotted (*IB*) and probed with anti-ASAP, Plk1, and α-actin (loading control) antibodies. For immunofluorescence analysis, asynchronous U-2 OS cells grown on coverslips were transfected with *GL2* or *Plk1* siRNAs or incubated with 1 μM TAL overnight. Cells were fixed in PAF/MTSB (*left panel*) or F/PHEM/methanol (*right panel*), probed with the polyclonal anti-ASAP (*green*) and the monoclonal anti-Plk1 antibody (*red*), and stained with Hoechst 33258 (*blue*) without (*left panel*) or after (*right panel*) MT depolymerization by incubation on ice for 60 min (*scale bar*, 10 μm). The percentage of mitosis with aberrant localization of ASAP is shown in the *table*. *B*, asynchronous U-2 OS cells were transfected with *GL2* or *γ-tubulin* siRNAs. Cell extracts were immunoblotted and probed with the anti-ASAP, anti-γ-tubulin, and α-actin (loading control) antibodies. For immunofluorescence analysis, cells were fixed in F/PHEM/methanol, probed with the polyclonal anti-ASAP (*green*) and the monoclonal anti-γ-tubulin antibody (*red*), and stained with Hoechst 33258 (*blue*) without (*left panel*) or after (*right panel*) MT depolymerization by incubation on ice for 60 min (*scale bar*, 10 μm). The percentage of mitosis with aberrant localization of ASAP is shown in the *table*. *C*, synchronized mitotic cells were immunoprecipitated (*IP*) with rabbit IgG or rabbit anti-ASAP antiserum, and precipitates were analyzed by immunoblotting with antibodies against ASAP and γ-tubulin (*Input*, 10% of protein extracts immunoprecipitated with 2 mg of protein extracts). *D*, centrosomes were isolated and enriched from U-2 OS cells using a discontinuous sucrose gradient (see "Materials and Methods"). *Left panel*, anti-ASAP and γ-tubulin antibodies were used for Western blot analysis. *Right panel*, centrosomes from fraction 2 were spun down onto coverslips and analyzed by immunofluorescence using the polyclonal anti-ASAP (*green*) and the monoclonal anti-γ-tubulin antibodies (*red*).

gets via the PBD (17, 18), the Plk1-ASAP interaction was almost completely abolished in cells co-transfected with Myc-Plk1-PBD mut (H538A/K540M) and FLAG-ASAP-WT (Fig. 1*D*). Collectively, these data suggest that ASAP and Plk1 co-localize and interact at spindle poles during mitosis and that this interaction requires specifically the PBD of Plk1.

Because ASAP also interacts with Aurora A, we then assessed whether ASAP, Aurora A, and Plk1 could be simultaneously co-immunoprecipitated. Aurora A and Plk1 were both detected in the ASAP immunoprecipitate (Fig. 1*E* and supplemental Fig. S1*C*). In synchronized cells, ASAP, Plk1, and Aurora A co-immunoprecipitation reached its maximum level at 13 h after release of the thymidine block (Fig. 1*F*, *right panel*), which corresponds to the mitotic peak, as indicated by the profile of both kinases whose expression level is highest during this phase (Fig. 1*F*, *left panel*).

Plk1 Promotes ASAP Recruitment to Centrosomes and Spindles through the γ-TuRC Pathway—We next investigated whether ASAP localization could be controlled by Plk1 or vice versa. Silencing either *ASAP* or *Plk1* by RNA interference (RNAi) did not alter the expression level of the other protein (Fig. 2*A*), and no significant effect on Plk1 localization was

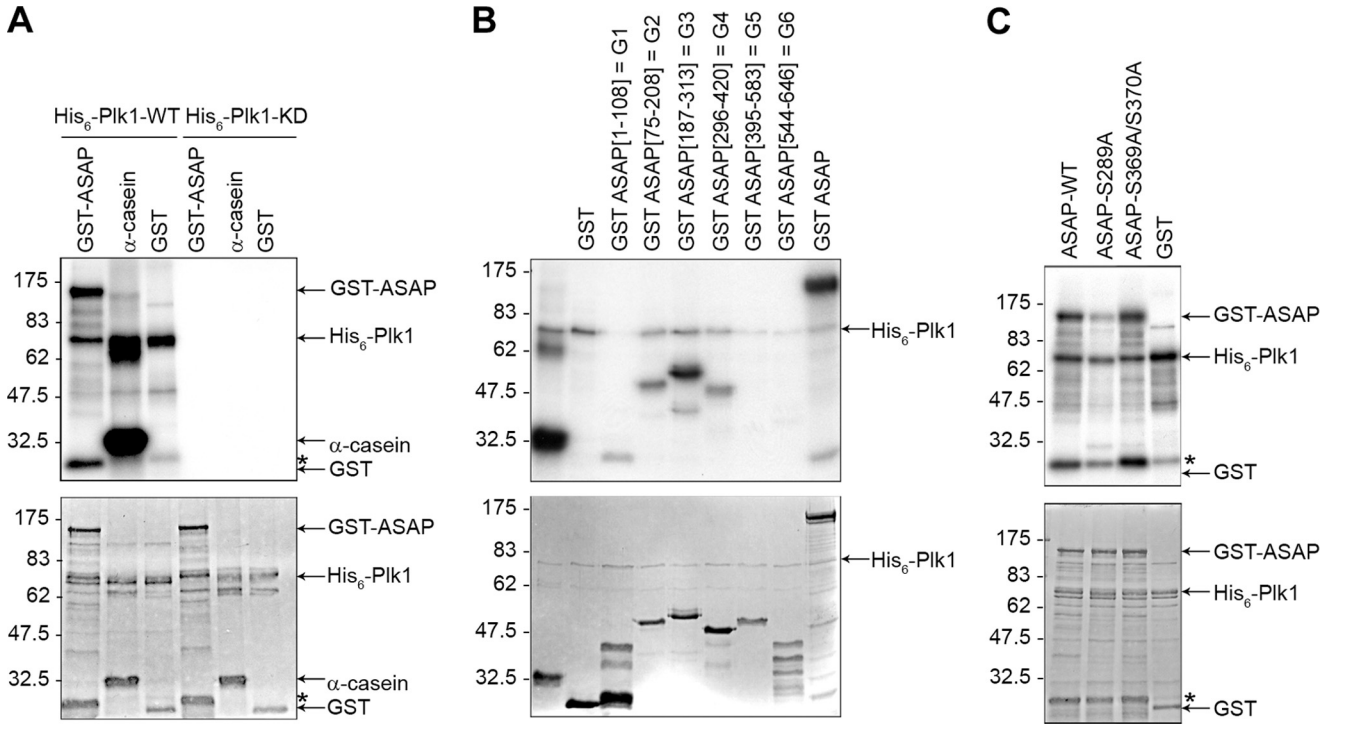

FIGURE 3. **Plk1 phosphorylates ASAP on S289 *in vitro*.** *A*, purified, recombinant GST-ASAP, α-casein, or GST was incubated with purified His_6-tagged wild-type Plk1 (His_6-Plk1-WT) or the kinase-dead mutant (N281A) (His_6-Plk1-KD) and [γ-^{32}P]ATP. The kinase reaction mixtures were then analyzed by SDS-PAGE and autoradiography (*upper panel*); the gel was also stained with Coomassie Blue (*lower panel*). *B*, purified GST, GST-ASAP fragments G1–G6 or GST-ASAP were used in a kinase assay with His_6-Plk1-WT as described in *A* and analyzed by SDS-PAGE and autoradiography (*upper panel*); the Coomassie Blue-stained gel is shown in the *lower panel*. *C*, *in vitro* kinase assays were performed using purified GST-ASAP, GST-ASAP mutants (S289A or S369A/S370A), or GST as described in *A* and analyzed by SDS-PAGE and autoradiography (*upper panel*); the Coomassie Blue-stained gel is shown in the *lower panel*.

observed in response to *ASAP* down-regulation (data not shown). However, *Plk1* depletion by RNAi caused defects in maturation and separation of centrosomes resulting in monopolar spindles (supplemental Fig. S2*A*), as described in previous reports (13, 33, 34), and prevented ASAP localization to both spindles (Fig. 2*A*, *left* immunofluorescence *panel*) and centrosomes as observed after cold MT depolymerization (Fig. 2*A*, *right* immunofluorescence *panel*). This suggests that Plk1 acts upstream of ASAP to promote ASAP localization to the spindle pole. The absence of effects of *Plk1* silencing on the localization of the spindle microtubule-associated protein (MAP) TPX2 and of Pericentrin (supplemental Fig. S2, *B* and *C*) indicates that the effect of Plk1 on ASAP localization is specific. As observed following *Plk1* knockdown, treatment with the Plk1 inhibitor TAL (30) also induced ASAP delocalization from the spindle and strongly decreased its presence at centrosomes, indicating that the kinase activity of Plk1 is required for ASAP localization to spindles and probably for enrichment at centrosomes during mitosis (Fig. 2*A* and supplemental Fig. S2*A*).

We have previously shown that ASAP depletion does not affect γ-tubulin recruitment to centrosomes. Because Plk1 also promotes γ-tubulin localization to centrosomes (35) (supplemental Fig. S2*D*), we hypothesized that ASAP recruitment might occur through the γ-TuRC pathway. We found that *γ-tubulin* depletion by RNAi also abolished ASAP localization to the mitotic spindle and also to centrosomes (Fig. 2*B*). Furthermore, in synchronized mitotic cells, γ-tubulin co-immunoprecipitated with ASAP (Fig. 2*C* and supplemental Fig. S1*D*). The co-localization to centrosomes of ASAP and γ-tubulin was further substantiated by biochemical approaches. Centrosomes from exponentially growing, unsynchronized U-2 OS cells were isolated and enriched using a discontinuous sucrose gradient. Western blotting and immunofluorescence revealed that ASAP and γ-tubulin were in the same centrosome-enriched fractions (Fig. 2*D*). NEDD1 has been reported to interact directly with and recruit γ-TuRC to centrosomes and spindle MTs to promote MT nucleation and spindle assembly (4, 5). This initially requires the Plk1 kinase activity (16). As expected, *γ-tubulin* and *NEDD1* gene depletion by RNAi induced abnormal monopolar spindles, but α-tubulin was still expressed (supplemental Fig. S2, *E* and *F*). Moreover, *NEDD1* gene down-regulation abolished ASAP localization to spindles and centrosomes (supplemental Fig. S2*F*), confirming the involvement of the Plk1-dependent recruitment of the γ-TuRC in ASAP localization at mitotic spindle poles.

Plk1 Phosphorylates ASAP on Serine 289 in Vitro—We next investigated whether ASAP was phosphorylated by Plk1. We performed *in vitro* kinase assays by incubating recombinant His_6-Plk1-WT or His_6-Plk1-KD (N181A) with recombinant GST-ASAP-WT. Marked phosphorylation of ASAP occurred in the presence of His_6-Plk1-WT, but not His_6-Plk1-KD. Plk1 did not phosphorylate recombinant GST alone, and we used α-casein as a positive control for the kinase assay (Fig. 3*A*). ASAP has 72 serine and 34 threonine residues, but phosphoamino acid analysis revealed that ASAP Plk1-dependent phosphorylation occurred on serine residues (supplemental Fig. S3*A*). To identify the ASAP domain(s) phosphorylated by Plk1, various GST-tagged ASAP fragments (G1–G6) were used

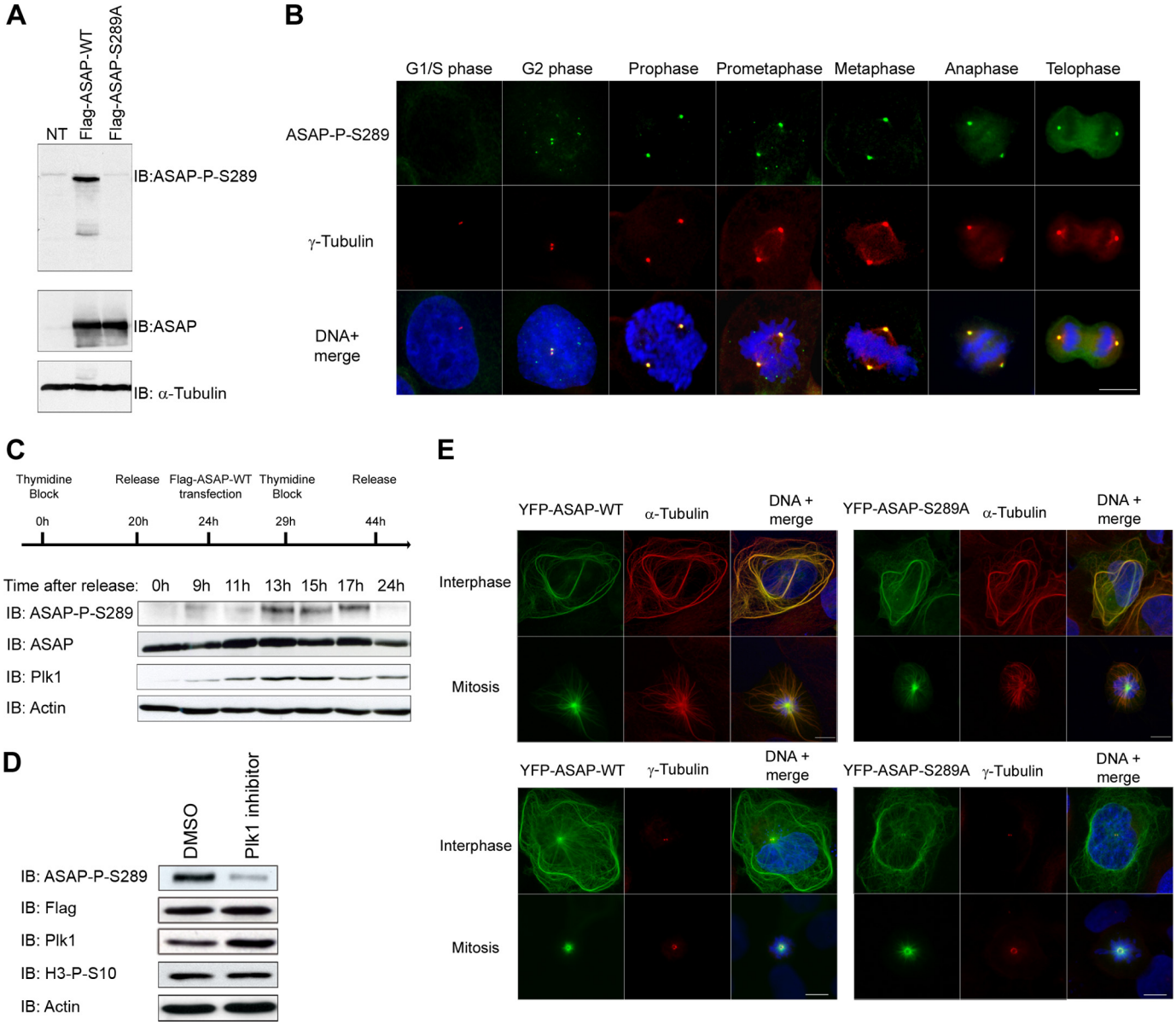

FIGURE 4. **Phosphorylation of ASAP at Ser-289 by Plk1 *in vivo* occurs at centrosomes during mitosis.** *A*, U-2 OS cell lysates transfected with FLAG-ASAP-WT or FLAG-ASAP-S289A were immunoblotted (*IB*) with the anti-ASAP-P-S289 (*left*) and anti-ASAP (*right*) antibodies. *NT*, nontransfected cells. α-Tubulin is shown as a loading control. *B*, asynchronous U-2 OS cells were grown on glass coverslips, fixed in F/PHEM/methanol, probed with the anti-ASAP-Ser(P)-289 (*green*) and anti-γ-tubulin (*red*) antibodies, and stained with Hoechst 33258 (*blue*); the different stages of the cell cycle are shown from G_2 to telophase (*scale bar*, 10 μm). *C*, U-2 OS cells were synchronized by double thymidine block and transfected with FLAG-ASAP during the first release, as indicated on the *schematic*. At the indicated time points after the second release, cells lysates were analyzed by immunoblotting using the indicated antibodies. α-Actin was used as a loading control. *D*, U-2 OS cells were transfected with FLAG-ASAP-WT, synchronized by thymidine block, and released in the presence of either dimethyl sulfoxide (*DMSO*) (control) or 1 μM TAL for 13 h. Cell extracts were immunoblotted with the anti-ASAP-Ser(P)-289, anti-FLAG, anti-Plk1, and anti-H3-Ser(P)-10 antibodies. α-Actin is shown as a loading control. *E*, U-2 OS cells were grown on glass coverslips, transfected with YFP-ASAP-WT (*left panels*) or YFP-ASAP-S289A mutant (*right panels*), fixed in PAF/MTSB (*upper panels*) or in F/PHEM/methanol (*lower panels*), and probed with anti-ASAP (*green*) and anti-α-tubulin (*red*) (*top*), anti-γ-tubulin (*red*) (*bottom*) and stained with Hoechst 33258 (*blue*) (*scale bar*, 10 μm).

for *in vitro* kinase assays. G3 fragment was strongly phosphorylated by Plk1 and to a lesser extent G2 and G4 (Fig. 3*B*). The G3 fragment contains the $ENS^{289}F$ sequence that is conserved in mouse and *Xenopus laevis* and resembles the Plk1 conserved consensus phosphorylation sequence E/D/Q)-*X*-(S/T)-Φ, where *X* denotes any amino acid and Φ denotes a hydrophobic amino acid (7). Phosphopeptide mapping of *in vitro* phosphorylated ASAP using mass spectrometry also identified Ser-289 as a potential phosphorylation site by Plk1 (supplemental Fig. S3*B*). This finding was confirmed by *in vitro* kinase assays showing that, differently from GST-ASAP-WT or the GST-ASAP-S369A/S370A mutant, the GST-ASAP-S289A mutant was not efficiently phosphorylated by Plk1 (Fig. 3*C*).

ASAP Phosphorylation on Serine 289 in Vivo Occurs at Centrosomes during Mitosis—To explore the functional significance of ASAP phosphorylation by Plk1, a polyclonal antibody was raised against Ser(P)-289 ASAP and affinity-purified. Ser(P)-289 recognized wild type ASAP but not the S289A mutant in protein extracts from U-2 OS cells transfected with FLAG-ASAP-WT and FLAG-ASAP-S289A (Fig. 4*A*). Western

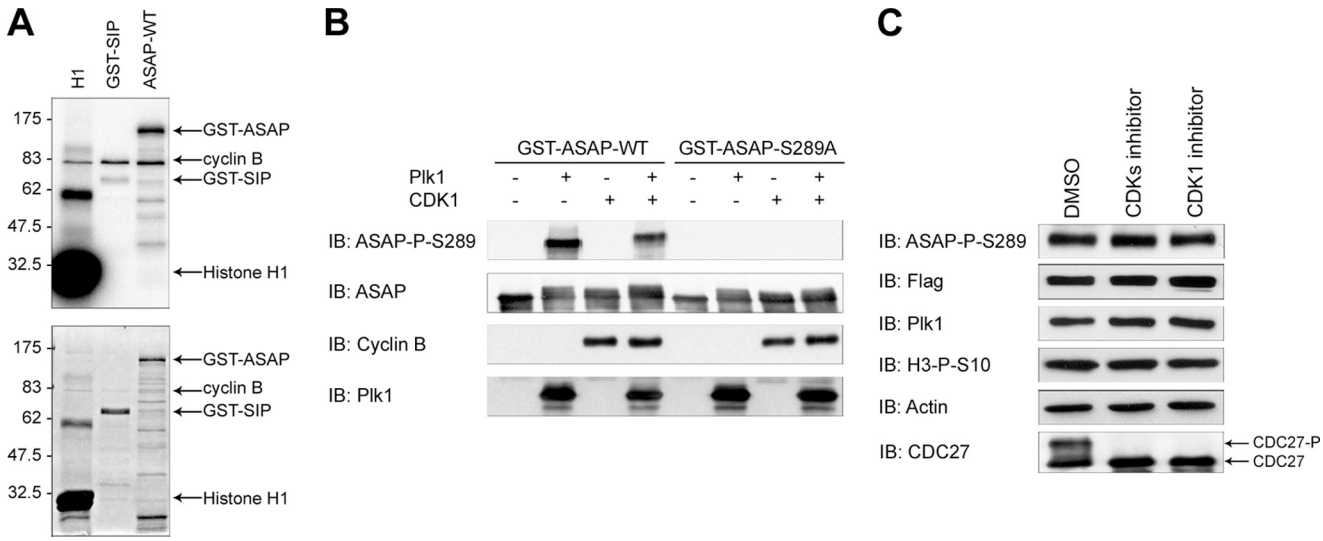

FIGURE 5. **Plk1-dependent phosphorylation of ASAP on serine 289 does not require a priming phosphorylation by Cdk1/Cyclin B *in vivo*.** *A*, purified GST-ASAP, histone H1 (positive control), or GST-SIP (negative control) was incubated with purified Cdk1/Cyclin B complex and [γ-^{32}P]ATP. The kinase reaction mixtures were then analyzed by SDS-PAGE and autoradiography (*upper panel*); the gel was also stained with Coomassie Blue (*lower panel*). *B*, purified GST-ASAP-WT or GST-ASAP-S289A mutant (negative control) was first incubated or not with Cdk1/Cyclin B complex for 30 min, treated with the CDK1 inhibitor RO-3306 for 10 min, and finally incubated with Plk1 for 30 min (see "Materials and Methods"). Reaction products were analyzed by SDS-PAGE and immunoblotted (*IB*) with anti-ASAP-Ser(P)-289, anti-ASAP, anti-Cyclin B, and anti-Plk1 antibodies as indicated. *C*, U-2 OS cells were transfected with FLAG-ASAP-WT, synchronized by thymidine block, and released for 16 h in the presence of nocodazole. Then, mitotic cells were recovered by mitotic shake-off and treated for 30 min with dimethyl sulfoxide (*DMSO*) (control), 50 μM roscovitine (CDK inhibitor), or 2 μM RO-3306 (CDK1 inhibitor). Cell extracts were immunoblotted with the anti-ASAP-Ser(P)-289, anti-FLAG, anti-Plk1, anti H3-Ser(P)-10 (mitotic marker) and anti-Cdc27 antibodies. The phosphoshift band of anti-Cdc27 is shown as a marker of Cdk activity. α-Actin was used as a loading control.

blot immunolabeling was abolished by prior dephosphorylation of immunoprecipitated FLAG-ASAP-WT by λ-phosphatase (supplemental Fig. S4*A*). Immunoprecipitation of overexpressed ASAP with the Ser(P)-289 antibody was also competitively inhibited by the phosphorylated immunogenic peptide but not by the unphosphorylated one (supplemental Fig. S4*B*). Unfortunately, the antibody was not sensitive enough to recognize endogenous ASAP in Western blots. We next investigated the subcellular localization of Ser(P)-289 ASAP in U-2 OS cells. The Ser(P)-289 form localized specifically to centrosomes, as shown by γ-tubulin co-labeling from late interphase to telophase (Fig. 4*B*). Again, labeling was lost following competition with the phosphorylated peptide but not with the unphosphorylated one (supplemental Fig. S4*C*). Moreover, the signal was also abolished following ASAP gene depletion (supplemental Fig. S4*D*), showing the specificity of this antibody. Immunofluorescence on synchronized cells analyzed at S, G_2, and M phases showed that Ser-289 labeling at interphase corresponded to cells in late G_2 (not shown). We confirmed by Western blotting that ASAP phosphorylation at Ser-289 is cell cycle-regulated, as phosphorylated ASAP was detected during mitosis, concomitant with the peak of Plk1 expression (Fig. 4*C*). In addition, the *Plk1* depletion by RNAi or the use of the Plk1 inhibitor TAL on nontransfected cells (supplemental Fig. S4, *E* and *F*) or on synchronized mitotic cells transfected with FLAG-ASAP-WT (Fig. 4*B*) confirming the specificity of this antibody abolished the Ser(P)-289 signal, indicating that it indeed depends on the Plk1 kinase activity.

To investigate whether phosphorylation of ASAP on Ser-289 by Plk1 was involved in ASAP localization, we examined the expression of YFP-ASAP-WT and YFP-ASAP-S289A in U-2 OS cells. YFP-ASAP-WT and YFP-ASAP-S289A showed identical expression patterns, with monopolar spindles and interphasic bundles, both hallmarks of ASAP overexpression (23) (Fig. 4*E* top), and localization at centrosomes at mitosis as indicated by the γ-tubulin staining (Fig. 4*E* bottom), showing that phosphorylation of ASAP on Ser-289 by Plk1 is not involved in its localization. This implies that either it depends only on the prior γ-TuRC recruitment to centrosomes, or it requires another Plk1 phosphorylation site.

Because ASAP is also phosphorylated by Aurora A on Ser-625, we checked whether the inhibition of one kinase would have an impact on the phosphorylation of the other. Given that ASAP is degraded by the proteasome upon *Aurora A* depletion by RNAi (24), we used the Aurora A-specific inhibitor MLN8054 (36) or the Plk1 inhibitor TAL, separately or together, on mitotic synchronized cells. MLN8054 did not induce ASAP degradation (supplemental Fig. S5*A*). Following inhibition of Aurora A activity, ASAP was still targeted to the centrosomes, thus excluding an involvement of Aurora A in this process (data not shown). We did not observe any effect on Ser-625 phosphorylation upon Plk1 inhibition or on Ser-289 phosphorylation following Aurora A inhibition in mitotic synchronized cells (supplemental Fig. S5, *A* and *B*). Treatment with both inhibitors reduced the Ser-289 and Ser-625 signal, as expected (supplemental Fig. S5, *A* and *B*).

ASAP Phosphorylation on Serine 289 Does Not Need Priming by Cdk1/Cyclin B—Several reports suggest that the PBD of Plk1 binds to a S[S/T]P motif on its targets. Cdk1/Cyclin B kinase activity is often responsible for priming the Plk1 docking sites during the first step of mitosis (17, 18). No strict consensus S[S/T]P motif was found in the ASAP sequence. However, although the optimal Cdk phosphorylation consensus sequence

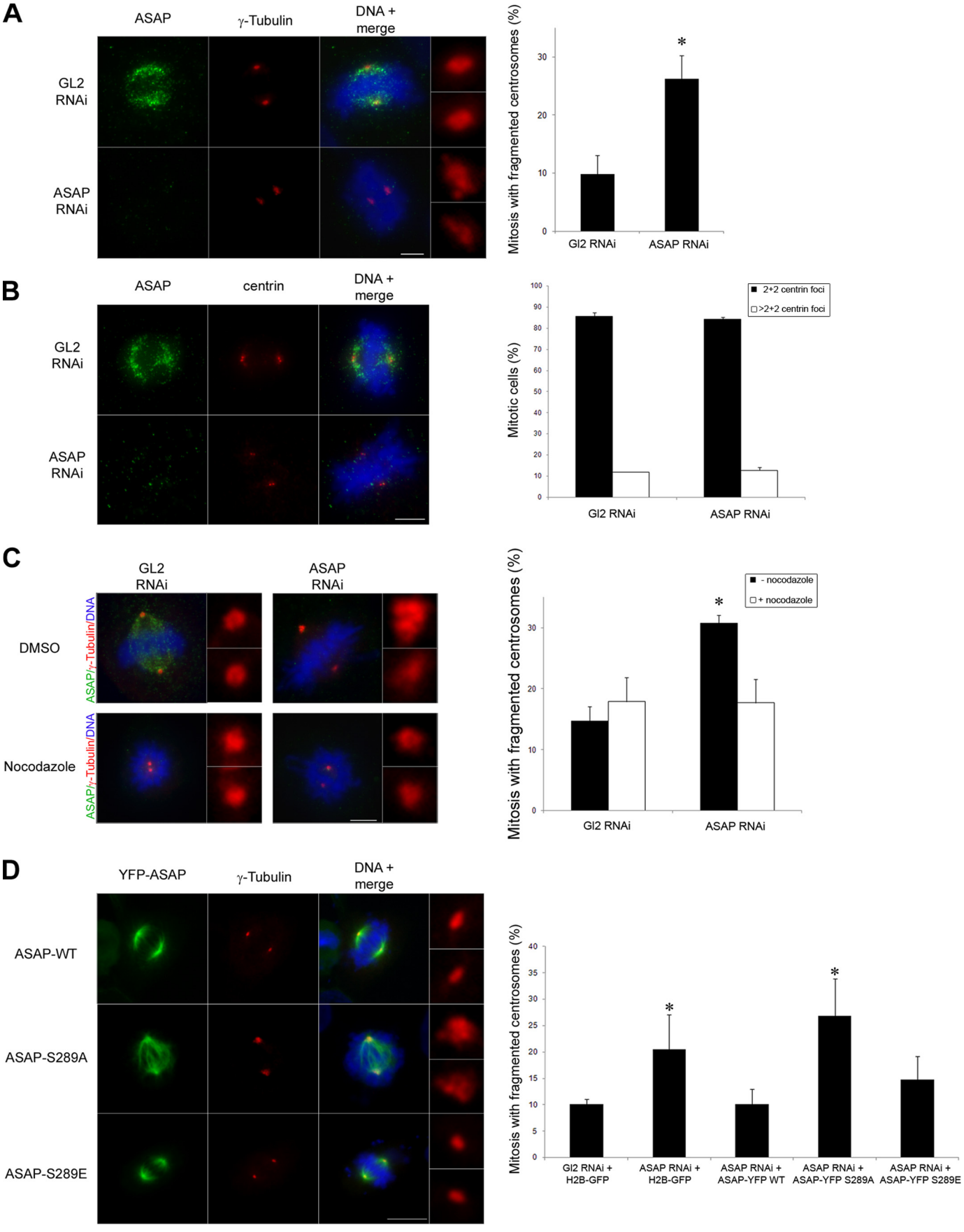
A
ASAP
γ-Tubulin
DNA + merge
GL2 RNAi
ASAP RNAi
Mitosis with fragmented centrosomes (%)
Gl2 RNAi
ASAP RNAi
B
ASAP
centrin
DNA + merge
GL2 RNAi
ASAP RNAi
Mitotic cells (%)
2+2 centrin foci
>2+2 centrin foci
Gl2 RNAi
ASAP RNAi
C
GL2 RNAi
ASAP RNAi
DMSO
Nocodazole
ASAP/γ-Tubulin/DNA
Mitosis with fragmented centrosomes (%)
- nocodazole
+ nocodazole
Gl2 RNAi
ASAP RNAi
D
YFP-ASAP
γ-Tubulin
DNA + merge
ASAP-WT
ASAP-S289A
ASAP-S289E
Mitosis with fragmented centrosomes (%)
Gl2 RNAi + H2B-GFP
ASAP RNAi + H2B-GFP
ASAP RNAi + ASAP-YFP WT
ASAP RNAi + ASAP-YFP S289A
ASAP RNAi + ASAP-YFP S289E

is ([ST]P*X*[KR]), 32% of Cdk1/Cyclin B phosphorylation sites identified in a large scale screening are suboptimal sites that contain only the minimal necessary proline feature [ST]P (37). Because such [ST]P motif is present in ASAP, it could function as a Cdk1/Cyclin B phosphorylation site. Indeed, GST-ASAP-WT was phosphorylated *in vitro* by recombinant Cdk1/Cyclin B, compared with GST-SIP, the negative control (Fig. 5*A*). We then performed a two-step *in vitro* sequential kinase assay with Cdk1/Cyclin B and His_6-Plk1-WT and GST-ASA-WT or GST-ASAP-S289A under saturating conditions. The band containing GST-ASAP-WT was obviously up-shifted in the presence of Cdk1/Cyclin B, confirming that ASAP might be phosphorylated by this complex. However, preincubation with Cdk1/Cyclin B did not further increase ASAP phosphorylation by Plk1, suggesting that the prephosphorylation by Cdk1/Cyclin B is not required for ASAP Ser-289 phosphorylation by Plk1 (Fig. 5*B*). To confirm this result *in vivo*, we have treated mitotic cells with the CDK inhibitor roscovitin or the CDK1 inhibitor RO-3306. The efficiency of the inhibitor was attested by the disappearance of the phosphorylated form of Cdc27, a mitotic substrate of Cdk1/Cyclin B. Because inhibition of Cdk1 induces mitotic exit, drugs were incubated for a short time, and the similar proportion of mitotic cells between samples was confirmed with the level of the mitotic marker, histone H3 phosphorylated on serine 10. Under these conditions, phosphorylation of ASAP on Ser-289 was not modified upon cell treatment with the CDK inhibitor roscovitin or the CDK1 inhibitor RO-3306 (Fig. 5*C*). Taken together, these results indicate that ASAP phosphorylation on Ser-289 by Plk1 is independent of a priming phosphorylation by the Cdk1/Cyclin B complex.

Phosphorylation of ASAP on Serine 289 Is Required for Centrosome Integrity during Mitosis—Previous results indicate that bipolar spindles, although abnormal, can form in the absence of ASAP (23). Proteins involved in MT dynamics, such as ASAP, may play a role in centrosome integrity as has recently been shown for members of the HAUS complex (38). Indeed, 72 h after transfection of *ASAP* siRNA in U-2 OS cells, we observed abnormal, fragmented centrosomes in bipolar mitotic spindles (Fig. 6*A*). The use of another PCM marker, the Pericentrin, confirmed this fragmentation phenotype (supplemental Fig. S6*A*). We previously missed this phenotype, probably because we analyzed cells earlier (48 h), in which ASAP silencing was not as complete as in the current experiments. Moreover, we did not observe defects in the number and in the structures labeled by the anti-γ-tubulin antibody in interphasic *ASAP*-depleted cells (supplemental Fig. S6*B*), indicating that the defects observed are indeed not due to an overduplication of the centrosomes in G_1/S. We next labeled *ASAP*-depleted cells with the anti-Centrin antibody. The absence of ASAP did not affect the number of centrioles in mitotic cells (Fig. 6*B*) or the distance between centrioles (not shown), suggesting that ASAP is not involved in their duplication or cohesion. Taken together, these data suggest that either ASAP is required for spindle pole integrity by preventing the fragmentation of the pericentriolar material or its depletion might generate an imbalance of forces within the spindle that centrosomes cannot sustain, ultimately leading to their fragmentation. To discriminate between these two possibilities, we investigated the effect of the microtubule-depolymerizing agent nocodazole on the fragmentation of mitotic centrosomes following *ASAP* down-regulation. Nocodazole treatment of cells transfected with *ASAP* siRNA reduced the number of cells with fragmented centrosomes to control levels (Fig. 6*C*), indicating that MTs are required for centrosomal fragmentation to occur. Fragmentation phenotype upon ASAP depletion was further confirmed using another PCM marker, the Pericentrin.

We then performed rescue experiments by co-transfecting *ASAP*-depleted cells with plasmids that express RNAi-refractory YFP-ASAP-WT, YFP-ASAP-S289A (nonphosphorylatable), or YFP-ASAP-S289E (phosphomimetic) mutants (Fig. 6*D* and supplemental Fig. S5*B*). One of the hallmarks of ASAP overexpression is a high proportion of monopolar spindles (23). This was also found when the YFP-ASAP-S289A or -S289E was overexpressed, because ~40% of the observed spindles were monopolar with a ring-shaped centrosome (data not shown), even though the quantity of overexpressed ASAP was as close as possible to endogenous levels. We thus decided to take into account only the bipolar spindles that correspond to a more physiological ASAP expression level. In contrast to the ASAP-S289A mutant, ASAP-WT and the phosphomimetic mutant ASAP-S289E largely rescued the spindle pole defects due to *ASAP* depletion (Fig. 6*D*). These data show that the ASAP role in the maintenance of spindle pole integrity we describe in this paper, depends, at least in part, on its phosphorylation on Ser-289 by Plk1.

FIGURE 6. **Phosphorylation of ASAP on Ser-289 contributes to spindle pole integrity.** *A*, *ASAP* depletion by RNAi leads to formation of abnormal centrosomes in mitosis. 72 h after *Luciferase GL2* or *ASAP* siRNA transfection in U-2 OS cells, centrosome phenotypes were analyzed by immunofluorescence (*left panels*) using the anti-ASAP (*green*) and anti-γ-tubulin antibodies (*red*) and Hoechst 33258 (*blue*) (*scale bar*, 5 μm). Enlargements (×4.5) of representative normal (*GL2* RNAi panel) or abnormal (*ASAP* RNAi panel) centrosomes are shown on the *right* of the *panels*. The number of mitotic cells with abnormal centrosomes was quantified (*right panel*). Data are shown as average ± S.E. (*error bars*) determined from four independent experiments (total of mitotic cells scored: 400). *, $p < 0.001$ by Student's *t* test. *B*, 72 h after *GL2* or *ASAP* siRNA transfection in U-2 OS cells, the phenotype of centrioles was analyzed by immunofluorescence (*left panels*) using the anti-ASAP (*green*) and anti-Centrin antibodies (*red*) and Hoechst 33258 (*blue*) (*scale bar*, 5 μm). The number of Centrin foci at poles of mitotic cells was quantified (*right panel*). Data are shown as average ± S.E. determined from three independent experiments (total mitosis scored: 400). *C*, 72 h after *GL2* or *ASAP* siRNA transfection, U-2 OS cells were incubated with dimethyl sulfoxide (*DMSO*) (control) or 50 ng/ml nocodazole for 6 h. *Left panels*, centrosome phenotypes were analyzed by immunofluorescence using the anti-ASAP (*green*) and anti-γ-tubulin antibodies (*red*) and Hoechst 33258 (*blue*) (*scale bar*, 5 μm). Enlargements (×4.5) of centrosomes are shown on the *right* of each *panel*. *Right panels*, the number of mitotic cells with abnormal centrosomes was quantified. The data are shown as average ± S.E. determined from four independent experiments (total mitosis scored: 400). *, $p < 0.001$ by Student's *t* test. *D*, U-2 OS cells were co-transfected with the *ASAP* siRNA and either with the control plasmid H2B-GFP or with the RNAi-refractory plasmids YFP-ASAP-WT, YFP-ASAP-S289A, or YFP-ASAP-S289E, as indicated. *Left panels*, cell phenotype was analyzed by immunofluorescence. U2-OS were grown on coverslips, fixed in F/PHEM/methanol, and co-stained using the anti-γ-tubulin antibody (*red*) and Hoechst 33258. Enlargements (×4.5) of representative centrosomes are shown on the *right* of the *panels* (*scale bar*, 10 μm). *Right panel*, abnormal centrosomes were quantified. Data are shown as average ± S.E. determined from three independent experiments (total mitosis scored: ~300). *, $p < 0.05$ by Student's *t* test.

DISCUSSION

Aneuploidy and chromosome instability are two of the most common abnormalities in cancer cells. They arise through defects in cell division and, specifically, through the unequal segregation of chromosomes between daughter cells during mitosis. Failure to form proper bipolar mitotic spindles, due to numeral as well as functional abnormalities of centrosomes, results in chromosome segregation errors (9, 39). Plk1 has been implicated in, among other mitotic functions, the regulation of centrosome maturation and cohesion (40) and in bipolar spindle assembly (7, 12). In this study, we show that the spindle- and centrosome-associated protein ASAP is localized to the spindle pole through a Plk1-dependent process. We have identified ASAP as a novel substrate of Plk1 and serine 289 as the major site of this phosphorylation. Moreover, we have confirmed its requirement for cell division and revealed that ASAP phosphorylated on serine 289 is involved in MT-dependent centrosome integrity.

Although centrosomal and spindle localization of ASAP requires Plk1, it does not depend on the Plk1 phosphorylation of ASAP on Ser-289. Given the huge number of Ser/Thr in ASAP, we cannot rule out that another Plk1 phosphorylation site might be involved in its localization. However, our results indicate that ASAP recruitment to the spindle pole is dependent on its interaction with γ-tubulin itself targeted to centrosomes by NEDD1 under the control of Plk1 (14, 16, 41). ASAP acts downstream of the above components because its depletion does not impair γ-tubulin, NEDD1, or Pericentrin localization. Through its interaction with γTuRC, NEDD1 promotes the nucleation of MTs from both centrosomes and the spindle (4, 5). Recent studies suggest that although Plk1 recruits NEDD1 to the centrosomes through direct interaction, it localizes NEDD1 to the spindle by interacting with and regulating FAM29A (14, 15). Similarly, the spindle and centrosomal localization of ASAP might depend on two pathways, one of which requires FAM29A. This hypothesis is reinforced by the role of FAM29A in preventing spindle pole fragmentation through MT dynamics (38). One could however imagine a function of ASAP, which needs further investigation, as a downstream effector of the FAM29A-NEDD1-γ-tubulin pathway in the regulation of MT dynamics.

We have identified Ser-289 as a major phosphorylation site of ASAP by Plk1 *in vivo*. Although priming phosphorylation strongly promotes docking of Plk1 to its targets, it may not be necessary for all interactions (20 and references therein). We show here that Plk1 PBD binding to ASAP is essential for the interaction between the two proteins (Fig. 1*D*) and that ASAP is probably phosphorylated *in vitro* by the Cdk1/Cyclin B complex as indicated by the up-shifted band (Fig. 5*A*). On the other hand, we demonstrate that ASAP phosphorylation at Ser-289 by Plk1 in G2/M does not require pre-phosphorylation by Cdk1/Cyclin B (Fig. 5, *B* and *C*). Of course, we cannot exclude the existence of another priming factor or the possibility that the interaction observed between ASAP and Plk1 is indirect and happens through another protein which is itself potentially primed by Cdk1/Cyclin B or another kinase. Thus, ASAP phosphorylation by the Cdk1/Cyclin B complex may have another function that needs to be deciphered. Nevertheless, we demonstrate that the regulation of Plk1 interaction with its substrates can vary, highlighting the relative importance of the different mechanisms used by Plk1 for regulating the activity of these substrates. We have determined that the phosphorylated fraction of ASAP is exclusively localized to the centrosome from G_2 to telophase. The timing of the onset of the Ser-289 phosphorylation and its localization suggest that it might be required at the beginning of mitosis. To understand the *in vivo* significance of this phosphorylation, we performed rescue experiments in *ASAP*-depleted cells. These presented a fuzzy and diffuse centrosome phenotype during mitosis, similar to those described after Kizuna or FAM29A depletion, two proteins regulated by Plk1 (38, 42). We have previously shown that ASAP controls MT stability and affects spindle bipolarity when overexpressed (23). Because ASAP does not induce monopolar spindles when depleted, we ruled out a direct role of ASAP in centrosome separation. Centriole duplication and cohesion or centrosome overamplification in interphase were not responsible for these phenotypes, showing that *ASAP* depletion induces PCM fragmentation during mitosis. However, any change in MT nucleation or MT stability should affect the pool of free tubulin and indirectly the dynamic properties of the spindle as a whole (43). Alternatively, an imbalance of forces on spindle MTs may cause spindle pole fragmentation in a MT-dependent fashion (38). Indeed, the centrosome fragmentation observed was MT-dependent, suggesting a change of MT dynamics upon ASAP depletion. However, this defect was clearly rescued by YFP-ASAP-WT or the phosphomimetic mutant YFP-ASAP-S289E but not by the ASAP-S289A mutant, suggesting that the Plk1-mediated phosphorylation of ASAP specifically strengthens spindle pole stability. Other proteins involved in MT dynamics are potential substrates or binding partners of Plk1. These include, for example, the MT-destabilizing proteins Op18/Stahmin1 (44) and TCTP (45), and the MT-depolymerizing Kif2A (46). Although we could not find a direct link between ASAP phosphorylation on Ser-289 and MT nucleation (data not shown), again we cannot exclude that the phenotype observed is only partial and would require the cumulative effect of several mutations to be complete and therefore stronger as is often described in the literature (16, 47). ASAP phosphorylation by Plk1 on Ser-289 may be required to maintain PCM integrity directly or indirectly via the regulation of other proteins involved in this process as proposed in Fig. 7.

Our previous study showed that ASAP phosphorylation on Ser-625 by Aurora A is required for correct spindle formation (24). The precise understanding of the cross-talk between Plk1 and Aurora A in ASAP regulation is made difficult because of the proteasome degradation of ASAP following *Aurora A* depletion by RNAi, which implies various technical constraints (24). We confirmed that ASAP, Plk1, and Aurora A interact during mitosis (Fig. 1*F*), but we could not demonstrate an impact of one kinase on the phosphorylation of the other, although Aurora A has been shown to activate Plk1 (21, 25), and Plk1 has been shown to promote Aurora A activity in a positive feedback loop (28). It is possible that in our conditions, there is still a basal Plk1 and Aurora A activity sufficient to phosphorylate ASAP but not high enough to allow mitosis entry. Although

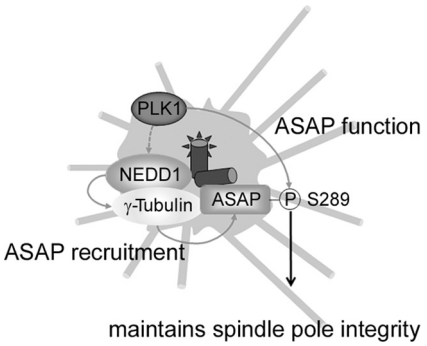

FIGURE 7. **Model for the role of Plk1-dependent ASAP phosphorylation in maintaining centrosome integrity.** Plk1 is a master regulator of centrosome maturation through phosphorylation and targeting of different PCM components. These various phosphorylations and interactions promote the recruitment of NEDD1, γ-tubulin, and ASAP to the centrosome. Plk1 binds to ASAP via its PBD (not shown) and phosphorylates ASAP on Ser-289. In the absence of Plk1-driven Ser-289 phosphorylation of ASAP, numeral and structural centrosome abnormalities occur, leading to abnormal mitotic spindle formation.

Plk1 is required for indirect targeting of ASAP to the spindle poles and for spindle pole integrity, Aurora A is necessary to stabilize ASAP and for spindle formation, suggesting specific contributions of both kinases in ASAP regulation and highlighting the fact that these kinases may have common substrates to regulate mitotic events finely. ASAP is a key mediator of mitosis and spindle assembly. The close relationship between ASAP and its regulators Aurora A and Plk1, combined with the mitotic defects observed following ASAP deregulation, clearly suggests that ASAP defects may contribute to the genetic instability commonly observed in most cancers.

In conclusion, our data identify ASAP, through its regulation by Plk1, as an essential and specific contributor to spindle pole function and spindle assembly in human cells. Increasing our knowledge of the mechanisms regulated by ASAP will undoubtedly help us to understand the processes that ensure faithful chromosome segregation and that are often deregulated in carcinogenesis and to consider new approaches for the development of anti-mitotic drugs.

Acknowledgments—We thank N. Lamb for helpful discussion, C. Berthenet for phosphoamino acid mapping, J. M. Saffin for centrosome purification, G. Poirier and S. Bourassa for phosphoproteomic analysis (Centre Protéomique, Laval, Canada), and J. Cau from the Montpellier RIO Imaging facility (Institut de Génétique Humaine). We thank the following researchers for providing essential reagents: R. H. Medema for the pRC-MYC-Plk1-WT plasmid, T. Lorca for the anti-Cdc27 antibody, A. Merdes for the anti-NEDD1 antibody, J. Salisbury for the anti-Centrin antibody, C. Prigent for the anti-Aurora A antibody, Bayer Schering Pharma AG for the Plk1 inhibitor, and J. Ecsedy and Millennium Pharmaceutical, Inc., for the Aurora A inhibitor. We thank E. Andermarcher for English language correction in the manuscript.

REFERENCES

1. Nigg, E. A. (2002) *Nat. Rev. Cancer* **2,** 815–825
2. Bettencourt-Dias, M., and Glover, D. M. (2007) *Nat. Rev. Mol. Cell Biol.* **8,** 451–463
3. Wiese, C., and Zheng, Y. (2006) *J. Cell Sci.* **119,** 4143–4153
4. Haren, L., Remy, M. H., Bazin, I., Callebaut, I., Wright, M., and Merdes, A. (2006) *J. Cell Biol.* **172,** 505–515
5. Lüders, J., Patel, U. K., and Stearns, T. (2006) *Nat. Cell Biol.* **8,** 137–147
6. Holland, A. J., and Cleveland, D. W. (2009) *Nat. Rev. Mol. Cell Biol.* **10,** 478–487
7. Barr, F. A., Silljé, H. H., and Nigg, E. A. (2004) *Nat. Rev. Mol. Cell Biol.* **5,** 429–440
8. Marumoto, T., Zhang, D., and Saya, H. (2005) *Nat. Rev. Cancer* **5,** 42–50
9. Fukasawa, K. (2007) *Nat. Rev. Cancer* **7,** 911–924
10. Zyss, D., and Gergely, F. (2009) *Trends Cell Biol.* **19,** 334–346
11. van de Weerdt, B. C., and Medema, R. H. (2006) *Cell Cycle* **5,** 853–864
12. Petronczki, M., Lénárt, P., and Peters, J. M. (2008) *Dev. Cell* **14,** 646–659
13. Sumara, I., Giménez-Abián, J. F., Gerlich, D., Hirota, T., Kraft, C., de la Torre, C., Ellenberg, J., and Peters, J. M. (2004) *Curr. Biol.* **14,** 1712–1722
14. Zhu, H., Coppinger, J. A., Jang, C. Y., Yates, J. R., 3rd, and Fang, G. (2008) *J. Cell Biol.* **183,** 835–848
15. Zhu, H., Fang, K., and Fang, G. (2009) *J. Cell Sci.* **122,** 2750–2759
16. Zhang, X., Chen, Q., Feng, J., Hou, J., Yang, F., Liu, J., Jiang, Q., and Zhang, C. (2009) *J. Cell Sci.* **122,** 2240–2251
17. Elia, A. E., Cantley, L. C., and Yaffe, M. B. (2003) *Science* **299,** 1228–1231
18. Elia, A. E., Rellos, P., Haire, L. F., Chao, J. W., Ivins, F. J., Hoepker, K., Mohammad, D., Cantley, L. C., Smerdon, S. J., and Yaffe, M. B. (2003) *Cell* **115,** 83–95
19. Lowery, D. M., Lim, D., and Yaffe, M. B. (2005) *Oncogene* **24,** 248–259
20. Archambault, V., D'Avino, P. P., Deery, M. J., Lilley, K. S., and Glover, D. M. (2008) *Genes Dev.* **22,** 2707–2720
21. Seki, A., Coppinger, J. A., Jang, C. Y., Yates, J. R., and Fang, G. (2008) *Science* **320,** 1655–1658
22. Park, J. E., Soung, N. K., Johmura, Y., Kang, Y. H., Liao, C., Lee, K. H., Park, C. H., Nicklaus, M. C., and Lee, K. S. (2010) *Cell. Mol. Life Sci.* **67,** 1957–1970
23. Saffin, J. M., Venoux, M., Prigent, C., Espeut, J., Poulat, F., Giorgi, D., Abrieu, A., and Rouquier, S. (2005) *Proc. Natl. Acad. Sci. U.S.A.* **102,** 11302–11307
24. Venoux, M., Basbous, J., Berthenet, C., Prigent, C., Fernandez, A., Lamb, N. J., and Rouquier, S. (2008) *Hum. Mol. Genet.* **17,** 215–224
25. Macùrek, L., Lindqvist, A., Lim, D., Lampson, M. A., Klompmaker, R., Freire, R., Clouin, C., Taylor, S. S., Yaffe, M. B., and Medema, R. H. (2008) *Nature* **455,** 119–123
26. Chan, E. H., Santamaria, A., Silljé, H. H., and Nigg, E. A. (2008) *Chromosoma* **117,** 457–469
27. Macùrek, L., Lindqvist, A., and Medema, R. H. (2009) *Cancer Res.* **69,** 4555–4558
28. Eckerdt, F., Pascreau, G., Phistry, M., Lewellyn, A. L., DePaoli-Roach, A. A., and Maller, J. L. (2009) *Cell Cycle* **8,** 2413–2419
29. Smits, V. A., Klompmaker, R., Arnaud, L., Rijksen, G., Nigg, E. A., and Medema, R. H. (2000) *Nat. Cell Biol.* **2,** 672–676
30. Santamaria, A., Neef, R., Eberspächer, U., Eis, K., Husemann, M., Mumberg, D., Prechtl, S., Schulze, V., Siemeister, G., Wortmann, L., Barr, F. A., and Nigg, E. A. (2007) *Mol. Biol. Cell* **18,** 4024–4036
31. Vigneron, S., Brioudes, E., Burgess, A., Labbé, J. C., Lorca, T., and Castro, A. (2009) *EMBO J.* **28,** 2786–2793
32. Moudjou, M. B. M., and Bornens, M. (1998) in *Cell Biology: A Laboratory Handbook* (Celis, J. E., ed) 2nd Ed., pp. 111–119, Academic, San Diego
33. Oshimori, N., Ohsugi, M., and Yamamoto, T. (2006) *Nat. Cell Biol.* **8,** 1095–1101
34. van Vugt, M. A., van de Weerdt, B. C., Vader, G., Janssen, H., Calafat, J., Klompmaker, R., Wolthuis, R. M., and Medema, R. H. (2004) *J. Biol. Chem.* **279,** 36841–36854
35. Hanisch, A., Wehner, A., Nigg, E. A., and Silljé, H. H. (2006) *Mol. Biol. Cell* **17,** 448–459
36. LeRoy, P. J., Hunter, J. J., Hoar, K. M., Burke, K. E., Shinde, V., Ruan, J., Bowman, D., Galvin, K., and Ecsedy, J. A. (2007) *Cancer Res.* **67,** 5362–5370
37. Blethrow, J. D., Glavy, J. S., Morgan, D. O., and Shokat, K. M. (2008) *Proc. Natl. Acad. Sci. U.S.A.* **105,** 1442–1447
38. Lawo, S., Bashkurov, M., Mullin, M., Ferreria, M. G., Kittler, R., Haber-

mann, B., Tagliaferro, A., Poser, I., Hutchins, J. R., Hegemann, B., Pinchev, D., Buchholz, F., Peters, J. M., Hyman, A. A., Gingras, A. C., and Pelletier, L. (2009) *Curr. Biol.* **19,** 816–826
39. Nigg, E. A. (2006) *Int. J. Cancer* **119,** 2717–2723
40. Wang, X., Yang, Y., Duan, Q., Jiang, N., Huang, Y., Darzynkiewicz, Z., and Dai, W. (2008) *Dev. Cell* **14,** 331–341
41. Haren, L., Stearns, T., and Lüders, J. (2009) *PLoS ONE* **4,** e5976
42. Oshimori, N., Li, X., Ohsugi, M., and Yamamoto, T. (2009) *EMBO J.* **28,** 2066–2076
43. Tillement, V., Remy, M. H., Raynaud-Messina, B., Mazzolini, L., Haren, L., and Merdes, A. (2009) *Biol. Cell* **101,** 1–11
44. Budde, P. P., Kumagai, A., Dunphy, W. G., and Heald, R. (2001) *J. Cell Biol.* **153,** 149–158
45. Yarm, F. R. (2002) *Mol. Cell. Biol.* **22,** 6209–6221
46. Jang, C. Y., Coppinger, J. A., Seki, A., Yates, J. R., 3rd, and Fang, G. (2009) *J. Cell Sci.* **122,** 1334–1341
47. Tamura, Y., Simizu, S., Muroi, M., Takagi, S., Kawatani, M., Watanabe, N., and Osada, H. (2009) *Oncogene* **28,** 107–116